

# Optical and structural properties of InGaN/GaN multiple quantum well structure grown by metalorganic chemical vapor deposition

Jeng-Hung Chen<sup>a</sup>, Zhe-Chuan Feng<sup>a,\*</sup>, Hung-Ling Tsai<sup>b</sup>, Jer-Ren Yang<sup>b</sup>, P. Li<sup>c</sup>,  
C. Wetzel<sup>c</sup>, T. Detchprohm<sup>c</sup>, J. Nelson<sup>c</sup>

<sup>a</sup> Graduate Institute of Electro-Optical Engineering and Department of Electrical Engineering, National Taiwan University, Taipei 106-17, Taiwan, ROC

<sup>b</sup> Department of Material Science and Engineering, National Taiwan University, Taipei 106-17, Taiwan, ROC

<sup>c</sup> Uniroyal Optoelectronics, Tampa, FL 33619, USA

Available online 26 September 2005

## Abstract

InGaN/GaN multiple quantum well light emitting diode structures have been grown on sapphire substrates by metalorganic chemical vapor deposition. They are investigated, in this study, by high-resolution X-ray diffraction, high-resolution transmission electron microscopy, photoluminescence, and photoluminescence excitation. HR-XRD showed multiple satellite peaks up to 10th order due to the quantum well superlattice confinement effects. These indicate the high quality of layer interface structures of this sample. Excitation power-dependent photoluminescence shows that both piezoelectric field-induced quantum-confined Stark effect and band filling effect influence the luminescent properties of this sample. Temperature-dependent photoluminescence of this sample has also been studied. The peak position of the PL exhibits a monotonic red-shift and the full width at half maximum of the PL band shows a W-shaped temperature-dependent behavior with increasing temperature. From the photoluminescence excitation results, a large energy difference, so-called Stokes shift, between the band-edge absorption and emission was observed.

© 2005 Elsevier B.V. All rights reserved.

**Keywords:** HR-XRD, high-resolution X-ray diffraction; HR-TEM, high-resolution transmission electron microscopy; PLE, photoluminescence excitation; MQW, multiple quantum well; MOCVD, metalorganic chemical vapor deposition

## 1. Introduction

Research and developments on GaN-based compound semiconductors and structures for optoelectronic and electronic applications have been very active in recent years. GaN and related III-nitride semiconductors possess large direct band gaps, extremely high hardness, very large heterojunction offsets, high thermal conductivity and high melting temperature, and great breakthroughs have been achieved in recent years for their materials growth and device manufactures in applications in blue-UV light emitting diode (LED), laser diode (LD) and other optoelectronic and electronic devices [1–7]. InGaN-based LED and LD grown on sapphire are now available commercially.

InGaN/GaN multiple quantum wells (MQWs) are attracting much research interest currently, acting as the active layer in above high brightness III-nitride LED and cw blue-green laser diode LD [1,8,9]. InGaN/GaN heterostructures can exhibit intense photoluminescence (PL) and electroluminescence (EL) despite of a high dislocation and defects density existed [10,11], and have advantages such as lowering the threshold current density for LDs and reducing the device sensitivity to temperature [12,13]. More research efforts have been made on InGaN/GaN multiple quantum wells; among which, most of InGaN/GaN MQWs were prepared by the metalorganic chemical vapor deposition (MOCVD) technique, which has been approved as a powerful technology for R&D and industry production of III-nitride materials and devices. This paper reports on the growth of InGaN–GaN MQW green LED structures on sapphire substrates. Analytical techniques of photoluminescence (PL), photoluminescence excitation (PLE), high-

\* Corresponding author. Tel.: +886 2 3366 3543; fax: +886 2 2367 7467.

E-mail address: [zcfeng@cc.ee.nut.edu.tw](mailto:zcfeng@cc.ee.nut.edu.tw) (Z.-C. Feng).

resolution (HR) X-ray diffraction (XRD) and transmission electron microscopy (TEM) have been employed to investigate their optical and structural properties.

## 2. Experimental details

The green light emitting diode, studied in this work, was grown on *c*-plane sapphire substrate by conventional MOCVD. Trimethylgallium (TMGa), trimethylindium (TMIn) and ammonia (NH<sub>3</sub>) were used as precursors. The carrier gas was H<sub>2</sub> and N<sub>2</sub>, respectively, for the growth of GaN and InGaN. Their structures were as follows: (0001) sapphire substrate, 30 nm low temperature (520 °C) grown GaN, 2 μm thick high temperature (HT) (1020 °C) grown GaN, a 800 nm InGaN layer followed by five periods of InGaN/GaN MQWs grown at 800 °C, 50 nm p-type AlGaIn and 150 nm HT-grown GaN cap layer. The structure consists of five-period MQWs with 4-nm InGaIn wells and 40-nm-thick GaN barriers. The average indium content was estimated to be 18%.

A Philips MRD high-resolution (HR) X-ray diffraction (XRD) including a five-crystal monochromator was used for characterization. The high-resolution transmission electron microscopy (HR-TEM) investigations were performed using a Philips CM 200 electron microscope with an acceleration voltage of 200 kV. For PL measurements, a cw He–Cd laser ( $\lambda=325$  nm) was used for PL excitation and a neutral density filter was used for controlling the excitation intensity. The samples to be measured were placed in a cryostat to control the ambient temperature. With circulated liquid helium, the cryostat could reach the lowest temperature of 9 K. PL photons from samples were then collected with a lens and guided into a monochromator through a fiber bundle. The PL signals were monitored with a lock-in amplifier. The tunable source of light was a 450 W Xenon lamp, dispersed by a 0.5 m spectrometer and the PL was dispersed by a 0.85 m double grating instrument for the PLE measurement.

## 3. Results and discussion

### 3.1. High-resolution X-ray diffraction measurement

Fig. 1 is the high-resolution X-ray diffraction (HR-XRD)  $\omega-2\theta$  scans for the (0002) reflection from this sample measured by a Philips MRD system. High order satellites up to 10th order can be clearly distinguished, which show very good InGaIn/GaN interfaces. The GaN peak localized at the angle of 17.28° is very sharp and all satellite bands are narrow. More fine structures are seen between satellite peaks. These indicate the excellent layer crystalline perfection and sharp interfaces between all multiple layers. Well/barrier width and average indium composition were estimated to be around 4.0 nm, 41.5 nm and 18%,

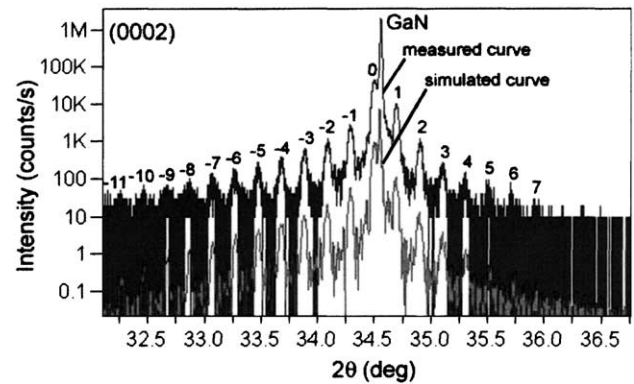


Fig. 1. HRXRD  $\omega-2\theta$  scans for the (0002) reflection from the five-period InGaIn/GaN green LED structures. The lower curve is the simulation from the Philips X'pert Smoothfit.

respectively, by using Philips X'pert Epitaxy and Smoothfit program.

### 3.2. High-resolution transmission electron microscopy

The high-resolution transmission electron microscopy (HR-TEM) investigations were performed with an acceleration voltage of 200 kV. All high-resolution micrographs were taken at Scherzer defocus, performed under short times of irradiation to prevent electron beam-induced artifacts [14]. Fig. 2 is the cross-sectional HR-TEM observation of the 5-QWs structure. Five QWs can be clearly identified in the image. The measured well and barrier widths are in good agreement with the XRD simulation. The dark contrast clearly shows that the QW is not uniform.

### 3.3. Excitation power-dependent photoluminescence

To investigate the luminescence mechanism, the excitation power-dependent PL measurement was carried out. Fig. 3 describes the excitation power dependence of PL spectra of this sample. With increasing excitation power from 0.07 to 33.1 mW, the emission shows a clear blue-shift. Fig. 4 shows the excitation power dependence of the emission peak energy (a) and linewidth full width at half maximum (FWHM) (b) of this sample. A blue-shift of  $\sim 163$  meV in the QW peak is evident in Fig. 4(a) as the excitation power increases from 0.07 mW to 33.1 mW. For the blue-shift of emission energy in this sample, normally, there are two possible explanations as mentioned in the introduction. One refers to the piezoelectric field-induced quantum-confined Stark effect (QCSE) [15,16], and another is related to the band-tailing effect due to the self-organized small In-rich regions [17,18]. In addition, in Fig. 3(b), the FWHM of the emission peak decreases with increasing excitation power from 0.07 to 3.2 mW, and then increases with increasing excitation power up to 33.1 mW. The anomalous excitation power dependence of the emission linewidth behavior is rarely in literature, but monotonous increasing or decreasing phenomena of the emission peak linewidth for InGaIn/GaN

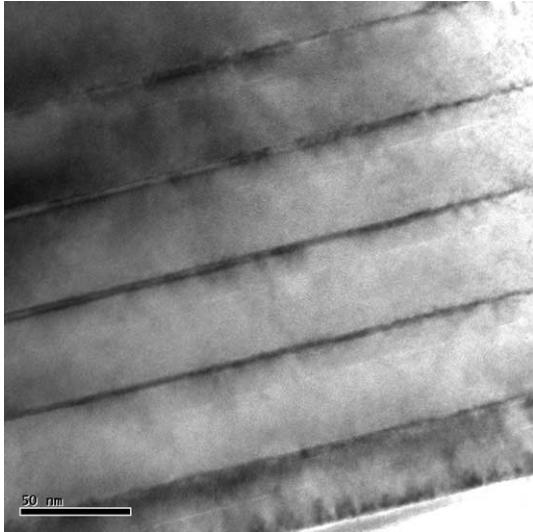


Fig. 2. HR-TEM micrograph of the InGaN/GaN MQW region.

QW structure were observed by another group [19–21]. These results can be well explained in terms of the QCSE along with the band filling effect. Due to the lattice mismatch between InGaN and GaN, the InGaN wells were under biaxial stress. In such a case, a piezoelectric field is induced since group III-nitrides have large piezoelectric constants along the (0001) orientation [22]. Therefore, the optical properties are strongly affected by this piezoelectric field, which produces QCSE. Due to the QCSE, the emission peak will show a red-shift and peak linewidth will be broadened, which has been observed earlier in the GaAs system [15,16]. The piezoelectric field can be screened by photo-generated carriers. The increase of the

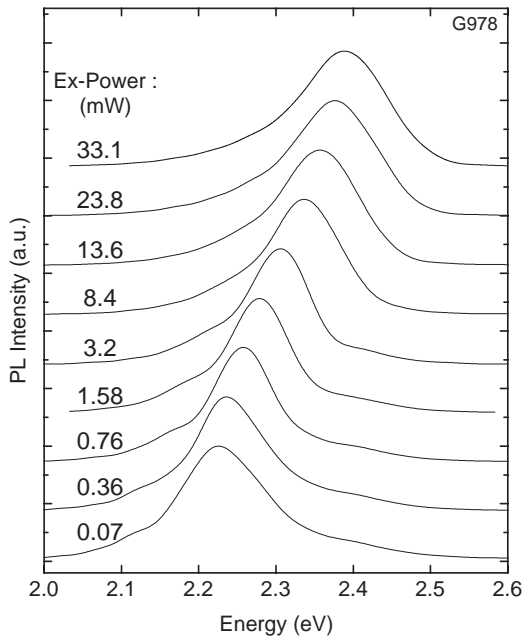


Fig. 3. Low temperature PL spectra of the InGaN/GaN 5-QWs structure measurement with different excitation intensities. All spectra are normalized and shifted vertically for clarity.

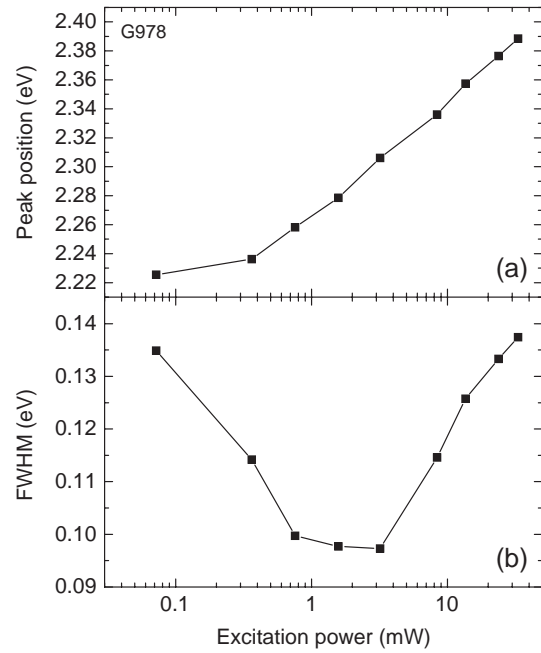


Fig. 4. Excitation power dependence of the peak position (a) and the FWHM (b) for the InGaN/GaN 5-QWs green LED structure.

excitation power from 0.07 to 3.2 mW weakens the QCSE and thus increases the transition energy, resulting in a blue-shift, and decreases the FWHM of the peak at the same time. At higher excitation power of more than 3.2 mW, the piezoelectric field seems to be fully screened, in which the linewidth does not decrease anymore. Then, the band filling was the dominant effect that can also cause the emission energy blue-shift. On the other hand, the band filling explains the broadening of the emission energy width. At high-level excitation, radiative recombination from high higher energy states will occur because there are more injected carriers and the possibility of higher energy states being filled with the excited carriers is larger. However, most of these excited carriers at the higher energy states relax to the ground states and the ground-state recombinations still dominate the PL emission, while only a small amount can directly recombine and emit light of larger energy. This can well explain the high excitation-dependent behavior of this sample.

### 3.4. Temperature-dependent photoluminescence

To further investigate the luminescence mechanism of this sample, the temperature-dependent PL measurement was also carried out. Fig. 5 shows the PL spectra for this sample in the temperature range from 9 to 300 K. In each case, the excitation power was ~23 mW. Single peak emission was observed at all temperatures, and the decrease of peak intensity is slow with an increase in temperature. Fig. 6 gives the peak position (a) and the FWHM (b) for the main emission peak as a function of temperatures obtained from Fig. 5. In general, with increasing temperature the

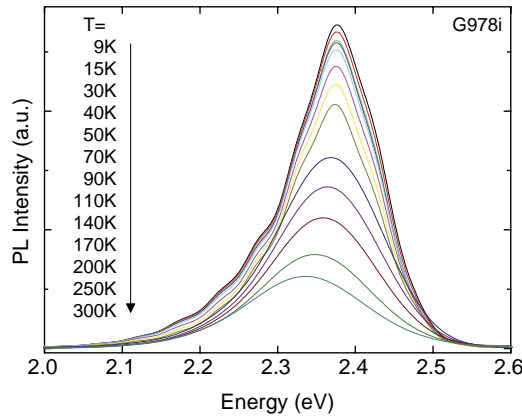


Fig. 5. The PL spectra for the InGaN/GaN 5-QWs green LED structure in the temperature range from 9 to 300 K.

band gap shrinks due to the temperature-dependent dilation of the lattice [24,25] and electron–lattice interaction. Thus, the peak position of PL spectrum exhibits only the red-shift. The empirical equation for this characteristic has been given by Varshni [26]:

$$E_g = E(0) - \frac{\alpha T^2}{T + \beta}$$

where  $E_g$  denotes the energy gap at temperature  $T$ ;  $E(0)$  at 0 K, and  $\alpha$  and  $\beta$  are constants. The constants  $\alpha$  and  $\beta$  are considered, in principle, to be dependent on the sample compositions, but independent of the growth method and the well width. The energy gap  $E_g$  variations with temperature are shown with the thin line together with the experimental data in Fig. 5. The values of  $\alpha$  and  $\beta$

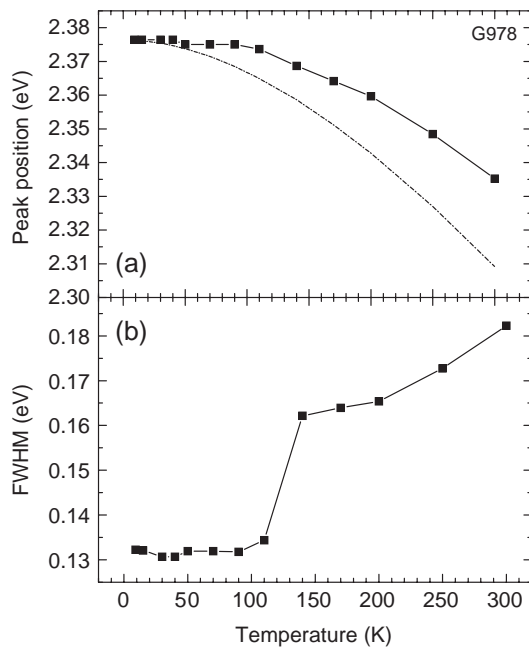


Fig. 6. Temperature dependence of the peak position (a) and the FWHM (b) for the InGaN/GaN 5-QWs green LED structure.

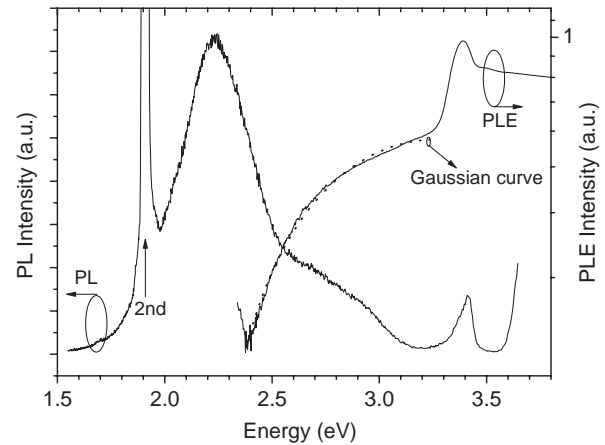


Fig. 7. PLE spectra at room temperature for the InGaN/GaN 5QW green LED structures and fits by the Gaussian.

were evaluated from the linear interpolation from the values for GaN and InN. The values of  $\alpha$  and  $\beta$  are 0.77 meV and 600 K for GaN [26] and 0.245 meV and 624 K for InN [27], respectively. The average indium content of 18% obtained from XRD simulation was used for the calculation.

The deviation of the PL peak position from the Varshni's characteristics is considered due to the thermal broadening of carrier distribution, the delocalization of carriers, the dissociation of the excitons, and the piezoelectric field intensity with temperature change.

Fig. 6(b) shows a W-shaped temperature dependence of the full width at half maximum (FWHM) of the PL band with a characteristic kink at about 140 K. The W-shaped temperature behavior of the linewidth is known to be a signature of exciton hopping over randomly dispersed localized states with a crossover from a non-thermalized to a thermalized distribution function of the excitons [28].

### 3.5. Photoluminescence excitation measurement

Fig. 7 shows PL and PLE spectra of these InGaN/GaN 5-QWs structures at room temperature. The most efficient excitation of the QW luminescence is achieved via the GaN barriers at energies above 3.5 eV, due to the fact that at most a few percent of the exciting light is directly absorbed in the quantum well. The high quality of the GaN layers can be inferred from the narrow excitonic absorption peak at the GaN absorption edge. In this case, we also found the large energy difference between the PLE absorption edge and the photoluminescence peak, that is, the Stokes shift. Both localization and the presence of the internal field are thought to influence the large Stokes shift between emission and absorption [29]. The large Stokes shifts confirmed that the luminescence center states were localized. We proposed that the localized states originate from the indium clusters caused by the fluctuation of the In concentration).

#### 4. Summary

In conclusion, we have reported on the MOCVD growth of InGaN/GaN multiple quantum well (MQW) green light emitting diode (LED) structures on sapphire substrates. Analytical investigation by photoluminescence, photoluminescence excitation, high-resolution X-ray diffraction and transmission electron microscopy has shown the excellent optical and structural properties. Up to 10th order QW XRD satellite peaks were observed. Transmission electron microscopy confirmed the sharp MQW structures and dimensional parameters. Detailed studies of luminescent properties have been performed via temperature- and excitation-dependent photoluminescence plus photoluminescence excitation measurements. The unique  $P$  and  $T$  behaviors of PL spectra are due to QCSE and filling effect of band-tail states within the MQW structures. A large Stokes shift was observed from the comparison of PL and PLE measurements. This penetrating investigation is helpful to better understand the luminescent mechanisms and find ways to further improve the material design and growth of InGaN/GaN MQWs for the wide spectral LED applications.

#### Acknowledgements

We acknowledge the help and support from Prof. Ian Ferguson, Alan Dolittle and C. C. Yang. The work at National Taiwan University was supported by funds from National Science Council of Republic of China, NSC 93-2218-E-002-011 and 93-2215-E-002-035.

#### References

- [1] S. Nakamura, S. Pearton, G. Fasol, *The Blue Laser Diode—The Complete Story*, Springer, Berlin, 2000.
- [2] J.I. Pankove, T.D. Moustakas ed., *Gallium Nitride (GaN) I and II, Semiconductors and Semimetals*, ed. R.K. Willardson and E.R. Weber, Vol. 50 and 58, Academic, San Diego, 1998 and 1999.
- [3] H. Morkoc, *Nitride Semiconductors and Devices*, Springer, Berlin, 1999.
- [4] S. Nakamura, S.G. Chichibu (Eds.), *Introduction to Nitride Semiconductor Blue Lasers and Light Emitting Diodes*, Taylor and Francis, London, 2000.
- [5] E.T. Yu, M.O. Manasreh ed., *III–V Nitride Semiconductors: Applications and Devices*, Vol. 16 in M.O. Manasreh ed., *Optoelectronic Properties of Semiconductors and Superlattices*, Taylor and Francis, New York, 2003.
- [6] M.O. Manasreh, I.T. Ferguson ed., *III–V Nitride Semiconductors: Growth*, Vol. 19 in M.O. Manasreh ed., *Optoelectronic Properties of Semiconductors and Superlattices*, New York, Taylor and Francis, 2003.
- [7] Zhe Chuan Feng, ed., *GaN-Based Materials: Growth and Characterization*, Imperial College Press, London, in press.
- [8] S. Nakamura, M. Senoh, S. Nagahama, N. Iwasa, T. Yamada, T. Matsushita, H. Kiyoku, Y. Sugimoto, T. Kozaki, H. Umemoto, M. Sano, K. Chocho, *Appl. Phys. Lett.* 72 (1998) 2014.
- [9] J.J. Song, W. Shan, in: B. Gil (Ed.), *Gallium Nitride and Related Semiconductors*, Michael Faraday House, 1998, p. 596.
- [10] Nakamura, S., Senoh, M., Nagahama, S., Iwasa, N., Yamada, T., Nukai, T., *Appl. Phys. Lett.*, 68 (1996) 3286; 69 (1996) 1477; 69 (1996) 4056.
- [11] K.S. Ramaiah, Y.K. Su, S.J. Vhang, B. Kerr, H.P. Liu, L.G. Chen, *Appl. Phys. Lett.* 84 (2004) 3307.
- [12] M. Koike, S. Yamasaki, S. Nagai, N. Koide, S. Asami, H. Amano, I. Akasaki, *Appl. Phys. Lett.* 68 (1996) 1403.
- [13] H. Gotoh, T. Tawara, Y. Kobayashi, N. Kobayashi, T. Saitoh, *Appl. Phys. Lett.* 83 (2003) 4791.
- [14] T.M. Smeeton, M.J. Kappers, J.S. Barnard, M.E. Vickers, C.J. Humphreys, *Appl. Phys. Lett.* 83 (2003) 5419.
- [15] D.A.B. Miller, D.S. Chemla, T.C. Damen, A.C. Gossard, W. Wiegmann, T.H. Woodand, C.A. Burrus, *Phys. Rev.*, B 32 (1985) 1043.
- [16] D.A.B. Miller, D.S. Chemla, T.C. Damen, A.C. Gossard, W. Wiegmann, T.H. Woodand, C.A. Burrus, *Phys. Rev. Lett.* 26 (1984) 2173.
- [17] Y. Narukawa, Y. Kawakami, M. Funato, S. Fujita, S. Nakamura, *Phys. Rev.*, B 55 (1997) 1938.
- [18] A. Statake, Y. Masmoto, T. Miyajima, T. Asatsuma, F. Nakamura, M. Ikeda, *Phys. Rev.*, B 57 (1998) R2041.
- [19] S. Khatsevich, D.H. Rich, X. Zhang, W. Zhou, P.D. Dapkus, *J. Appl. Phys.* 95 (2004) 1832.
- [20] T. Wang, D. Nakagawa, M. Lachab, T. Sugahara, S. Sakai, *Appl. Phys. Lett.* 74 (1999) 3128.
- [21] T. Wang, D. Nakagawa, J. Wang, T. Sugahara, S. Sakai, *Appl. Phys. Lett.* 73 (1998) 3571.
- [22] T. Takeuchi, S. Sota, M. Katsuragawa, M. Komori, H. Takeuchi, H. Amano, I. Akasaki, *Jpn. J. Appl. Phys.*, Part 2 36 (1997) L382.
- [24] R. M $\ddot{o}$ glich, R. Rompe, *Z. Phys.* 119 (1942) 492.
- [25] J. Bardeen, W. Shockley, *Phys. Rev.* 80 (1950) 72.
- [26] M.E. Levinstein, S.L. Rumyantsev, M.S. Shur, *Properties of Advanced Semiconductor Materials*, Wiley, New York, 2001, p. 4.
- [27] Q. Guo, A. Yoshida, *Jpn. J. Appl. Phys.* 33 (1994) 2453.
- [28] Kazlauskas, G. Tamulaitis, A. ukauskas, M.A. Khan, J.W. Yang, J. Zhang, G. Simin, M.S. Shur, R. Gaska, *Appl. Phys. Lett.* 83 (2003) 3722.
- [29] Jin Seo Im, Sabine Heppel, Holger Kollmer, Alexander Sohmer, Jurgen Off, Ferdinand Scholz, Andreas Hangleiter, *J. Cryst. Growth* 189/190 (1998) 597.